Theoretical Chemistry Accounts (2020) 139:127
https://doi.org/10.1007/s00214-020-02640-w

REGULAR ARTICLE

Photochemical activation of carbon dioxide in $Mg^+(CO_2)(H_2O)_{0,1}$

Tobias F. Pascher[1] · Erik Barwa[1] · Christian van der Linde[1] · Martin K. Beyer[1] · Milan Ončák[1]

Received: 3 April 2020 / Accepted: 20 June 2020 / Published online: 4 July 2020

Abstract
We combine multi-reference ab initio calculations with UV–VIS action spectroscopy to study photochemical activation of CO_2 on a singly charged magnesium ion, $[MgCO_2(H_2O)_{0,1}]^+$, as a model system for the metal/ligand interactions relevant in CO_2 photochemistry. For the non-hydrated species, two separated Mg^+ 3*s*–3*p* bands are observed within 5.0 eV. The low-energy band splits upon hydration with one water molecule. $[Mg(CO_2)]^+$ decomposes highly state-selectively, predominantly via multiphoton processes. Within the low-energy band, CO_2 is exclusively lost within the excited state manifold. For the high-energy band, an additional pathway becomes accessible: the CO_2 ligand is activated via a charge transfer, with photochemistry taking place on the CO_2^- moiety eventually leading to a loss of CO after absorption of a second photon. Upon hydration, already excitation into the first and second excited state leads to CO_2 activation in the excited state minimum; however, CO_2 predominantly evaporates upon fluorescence or absorption of another photon.

Keywords Photoactivation · Carbon dioxide activation · Multi-reference calculations · Spectroscopy

1 Introduction

The accurate theoretical description of electronically excited states remains a very difficult but important task for many applications including photocatalysis, [1] light harvesting, [2] photostability, [3, 4] photosensitizers, [5–9] and many more [10]. Already the description of absorption spectra might represent a challenge, e.g., when Rydberg states or charge-transfer excitations are encountered [10]. The complexity is further enhanced outside the Franck–Condon (FC) region, where single-reference methods become insufficient due to state crossings and more demanding multi-reference methods are needed [10–12]. Accurate description of conical intersections (CIs) represents an important task for the understanding of photochemical processes [13–16]. Another layer of difficulty is added in the case of theoretical investigations of metal complexes due to the presence of near-degenerate electronic states and relativistic effects [17].

Catalysis on metals has become a large focus in research due to their importance in, e.g., ammonia and methanol synthesis, [18, 19] but also for photoactivation [1, 20]. Due to its atmospheric relevance, especially activation and transformation of carbon dioxide are addressed in an increasing number of recent studies [21–23]. The direct charge transfer of an electron onto CO_2 forming an activated bent CO_2^- could be a key step in the activation process. However, the CO_2^- ion itself is metastable [24–27] and has to be hydrated or attached to a metal center to gain stability [28–31]. Only recently, we revealed that hydration of only three water molecules already leads to activation of carbon dioxide forming a CO_2^- ligand on a Mg^{2+} core [32, 33]. The combination of theory and UV–VIS spectroscopy provides a powerful tool for characterization of complicated processes in ionic metal complexes upon excitation [34]. With this approach, we investigated copper formate clusters relevant for carbon dioxide activation on copper centers in the ground state as well as electronically excited states [35–37].

Due to their intriguing charge-transfer chemistry in the ground state, hydrated magnesium ions $Mg^+(H_2O)_n$ have

Published as part of the topical collection of articles from the 17th edition of the Central European Symposium on Theoretical Chemistry (CESTC 2019) in Austria.

Electronic supplementary material The online version of this article (https://doi.org/10.1007/s00214-020-02640-w) contains supplementary material, which is available to authorized users.

✉ Martin K. Beyer
martin.beyer@uibk.ac.at

✉ Milan Ončák
milan.oncak@uibk.ac.at

[1] Institut für Ionenphysik und Angewandte Physik, Universität Innsbruck, Technikerstraße 25, 6020 Innsbruck, Austria

been studied extensively by theory and experiment [38–46]. Photodissociation spectroscopy of hydrated magnesium ions, $Mg^+(H_2O)_n$, provides a suitable model system and benchmark tool for theoretical calculations to investigate the hydrogen production on metal centers [47–51]. Theoretical investigations of Mg^+ complexes go back to 1991 [52, 53]. Already in 1993, the group of Duncan found partial CO loss in $[Mg(CO_2)]^+$ after excitation within one of the two separated 3*s*–3*p* excitation bands of Mg^+, pointing toward activation of carbon dioxide within the excited state [54–56]. Whereas the character, vibrational assignment and splitting of these bands was well understood, the photochemical process leading to the activation of the CO_2 ligand remained unclear due to computational limitations.

Here, we combine investigation of the excited state PES with photodissociation experiments in the gas phase to analyze the photochemical activation of CO_2 on a Mg^+ core with and without an additional water molecule.

2 Experimental and theoretical methods

The experimental gas-phase action spectra are obtained using FT-ICR mass spectrometry with the cell cooled to the temperature of about 80 K, see Supporting Information for details. For quantum chemical calculations, we used the molecular structures published in Ref. [32] as a starting point. Structures in the ground electronic state are modeled using the Coupled Cluster Singles and Doubles, CCSD/aug-cc-pVDZ, level of theory. For excited state calculations, Equation of Motion CCSD, EOM-CCSD/def2TZVP, and Multi-reference Configuration Interaction, MRCI/def2TZVP, single-point calculations are applied. The def2TZVP basis set is sufficient to describe the orbitals participating in the photochemistry of the system as no Rydberg states are observed among the low-lying excitations. An active space of seven electrons in nine orbitals (7,9) was employed. It includes the valence 3*s* electron of Mg^+ and six electrons of the CO_2 ligand which are important for description of the bending coordinate; nine orbitals allow for inclusion of up to six doublet electronic states. Relaxed excited state potential energy surface scans are performed on the Complete Active Space Self-Consistent Field, CASSCF/def2TZVP, level of theory. In comparison with EOM-CCSD, optimization on the CASSCF(7,9)/def2TZVP level of theory yields reasonable structures with similar minima. MRCI(7,9) single-point calculations are performed to include dynamic correlation.

For spectra modeling, we used Franck–Condon simulations [57, 58] as well as the linearized reflection principle within the harmonic approximation [59–61] at the EOM-CCSD/aug-cc-pVDZ level of theory. The Gaussian 16 software was employed for CCSD and EOM-CCSD calculations [62], the Molpro software package for CASSCF and MRCI calculations [63, 64].

3 Results and discussion

3.1 UV/VIS spectroscopy

We start our analysis with the spectrum of $[Mg(CO_2)]^+$ from the group of Duncan illustrated in Fig. 1a. At 3.66 eV, a vibrationally resolved absorption band was observed, along with the flank of a second peak at about 4.66 eV [54, 56]. With our tunable OPO system, we have spectral access to the full second absorption, for which we observe a band with a maximum at 4.88 eV, which is fitted very well with a single Gaussian. The resolved vibrational progression in the low-energy band indicates excitation into a bound state while the structureless high-energy band suggests no excited state minimum in the vicinity of the Franck–Condon point in

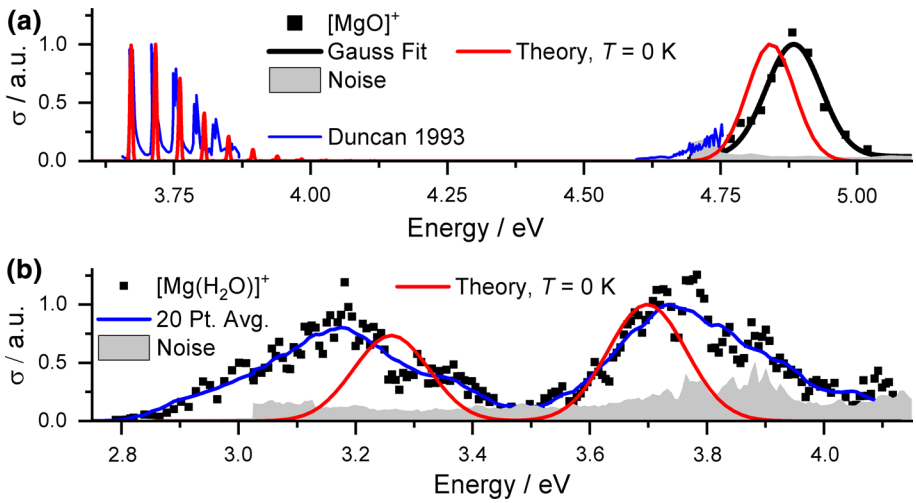

Fig. 1 Experimental photodissociation and modeled absorption spectra for (**a**) $[Mg(CO_2)]^+$ and (**b**) $[Mg(CO_2)(H_2O)]^+$. For modeling, Franck–Condon simulations shifted by 0.046 eV are used for the low-energy band in (**a**), the linearized reflection principle otherwise. The EOM-CCSD/aug-cc-pVDZ//CCSD/aug-cc-pVDZ approach was employed. Data for the blue curve in (**a**) are taken from Ref. [54]

this state. Based on these assumptions, we modeled the spectrum in Fig. 1a. The calculated bands are shifted to slightly lower energies by about 0.05 eV. The vibrational resolution due to the CO_2 stretching vibration at 360 cm^{-1} in the low-energy band yields a very good agreement between experiment and theory in the population of states even within the harmonic approximation. The width of the high-energy peak is well reproduced within the linearized reflection principle approximation.

Figure 1b shows spectral changes upon hydration in the $[Mg(CO_2)(H_2O)]^+$ ion. Weak fragment signals corresponding to loss of CO_2 were obtained in the range from 2.8 to 4.2 eV, where two well-separated bands with similar intensities are observed with maxima around 3.2 and 3.7 eV. Their shape is rather broad, which does not suggest excitation into a bound state near the FC point. Modeling of the spectra based on the linearized reflection principle at $T = 0$ K yields good agreement in excitation energies, with discrepancies smaller than 0.1 eV. However, the experimental width is significantly larger, almost by a factor of two. This points toward thermal effects playing an important role, with a more floppy ground state minimum compared to the case of bare $[Mg(CO_2)]^+$. To improve spectrum modeling, path integral molecular dynamics simulation on the CCSD potential energy surface would be possibly needed, lying beyond the scope of the present study.

3.2 Photochemistry

Decomposition pathways in $[Mg(CO_2)]^+$ highly depend on the investigated band. While for the first band, only CO_2 loss (reaction (1) in Table 1) was reported by the group of Duncan [54–56], CO loss was observed additionally (reaction (2)) in the flank of the high-energy band. Here, the branching ratio shifted in favor of $[MgO]^+$ and reaction (2) toward higher energies [54]. In line with this observation, we only detected the CO loss channel for the high-energy band, suggesting it is the predominant decomposition channel. Presumably due to the poor signal-to-noise ratio in our experiment, we could not detect the competing Mg^+ fragment reported by Duncan.

Table 1 Possible decomposition channels shown in Fig. 1 and Figure S1 with the calculated reaction energy ΔE

Reaction	Reactant	Products	ΔE/eV
(1)	$[Mg(CO_2)]^+$	$Mg^+ + CO_2$	0.65
(1*)		$Mg^{*+} + CO_2$	4.97
(2)		$[MgO]^+ + CO$	4.52
(3)	$[Mg(CO_2)(H_2O)]^+$	$[Mg(H_2O)]^+ + CO_2$	0.48
(3*)		$[Mg(H_2O)]^{*+} + CO_2$	3.98
(4)		$[Mg(CO_2)(OH)]^+ + H$	2.16
(5)		$[MgO(H_2O)]^+ + CO$	2.51
(6)		$[Mg(OH)]^+ + H + CO_2$	3.58
(7)		$[Mg(CO_2)]^+ + H_2O$	1.10

*Denotes the first excited state. Calculated at the CCSD/aug-cc-pVDZ level along with excitations at the EOM-CCSD/def2-TZVP level of theory

Upon hydration, excitation within the first two absorption bands leads only to CO_2 molecule loss, reaction (3). This is energetically the most favorable decomposition channel in the ground state, which suggests internal conversion. When the pulse energy is tripled and the number of laser pulses is doubled, $[Mg(CO_2)(OH)]^+$, $[MgO(H_2O)]^+$ and $[Mg(OH)]^+$ fragments are observed in smaller amounts starting at about 3.6 eV, see Figure S1. The respective reactions (4–6) would be accessible in the ground state with the available energy after internal conversion. However, the energetically preferred water evaporation is not observed, reaction (7). The observed pulse energy dependence and missing water loss in the experiment thus suggest the involvement of multiphoton processes.

We start our theoretical photochemical investigation with the linear $[Mg(CO_2)]^+$ complex. In the FC point, the singly occupied molecular orbital in the ground state is the 3*s* orbital of Mg^+ which is slightly perturbed by the CO_2 ligand (Fig. 2a). The first excitations correspond to the excitation of the 3*s* electron into $3p_{x,y}$ orbitals of Mg^+ with a vertical excitation energy of 3.70 eV (MRCI(7,9)/def2TZVP//CCSD/aug-cc-pVDZ) in the FC point. These are shifted from three 3*s*–3*p* transitions of bare Mg^+ at 4.31 eV (MRCI(1,4)/def2TZVP) due to destabilization of the 3*s* orbital upon binding of CO_2. The excitation at 4.93 eV (MRCI(7,9)/def2TZVP//CCSD/aug-cc-pVDZ) corresponds to excitation into the significantly perturbed $3p_z$ orbital of Mg^+, which is collinear with the CO_2 ligand. This is consistent with previous interpretation and the similar case of $[Mg(H_2O)]^+$ [47, 49, 54–56].

To investigate whether the observed dissociation pathway involving CO loss can be explained by electron transfer from Mg^+ to the CO_2 molecule, we performed a relaxed scan along the CO_2 angle for the D_1 and D_3 states on the MRCI(7,9)/def2TZVP//CASSCF(7,9)/def2TZVP level of theory in Fig. 2a, b, respectively.

The D_1 minimum in the direct vicinity of the FC point lies only 0.08 eV below the D_1 excitation energy, still with a linear CO_2 molecule and minimal structural changes. This minimum is well separated with a barrier of about 0.48 eV from an energetically lower-lying D_1 minimum where CO_2 is activated with an O–C–O angle of about 130°. Here, the electron is transferred from the Mg^+ center to the antibonding π^* orbital of the CO_2 ligand. During the charge transfer, the originally degenerate $3p_{x,y}$ orbitals split. According to the vibrationally resolved experimental spectrum for D_1, the D_1 minimum with bound linear CO_2 is the target state. However, fluorescence from this minimum can only

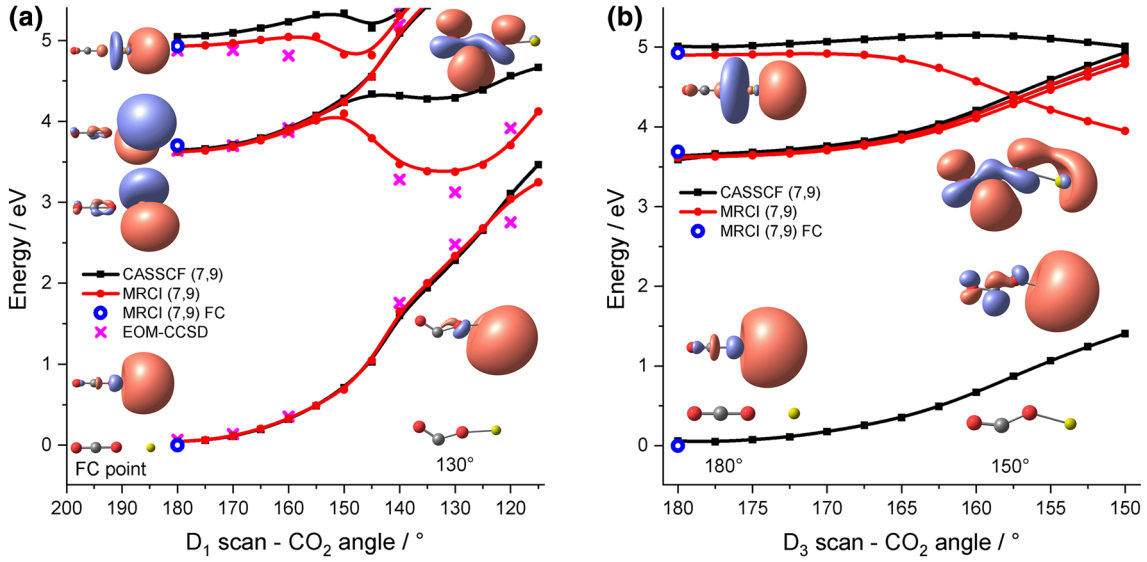

Fig. 2 Relaxed PES scan of the CO_2 angle in $[Mg(CO_2)]^+$ for (**a**) D_1 and (**b**) D_3 states at the CASSCF(7,9)/def2-TZVP and MRCI(7,9)//CASSCF(7,9)/def2-TZVP levels. FC point transition energies are given at the MRCI(7,9)/def2-TZVP//CCSD/aug-cc-pVDZ level. EOM-CCSD/def2-TZVP//CASSCF(7,9)/def2-TZVP energies are provided around the minima in (**a**). The structures and the most important singly occupied orbitals according to CASSCF CI vectors are shown for selected points

provide an energy of 0.12 eV, which is insufficient for the CO_2 loss observed according to reaction (1). Similarly, CO_2 loss within the excited state via reaction (1*) lies too high in energy, requiring 4.97 eV in total. The ground and the excited state manifold are well separated, and no curve crossing seems to be accessible.

However, a D_1 minimum can be reached after excitation into the D_3 state without any barrier (Fig. 2b), which corresponds to a charge-transfer complex between an activated, bent CO_2^- radical anion and Mg^{2+}. This observation is consistent with the experimental structureless absorption band suggesting a dissociative shape of the PES around the FC point for excitation into D_3. Orbital analysis of the relaxed structure in Fig. 2b confirms that the singly occupied $3p_z$-orbital of Mg^+ mixes with the antibonding π^* orbital of the carbon dioxide ligand upon bending. In the D_1 minimum, the electron is fully transferred from Mg^+ to the antibonding π^* orbital of the CO_2 molecule, the C–O bonds are slightly weakened (the one next to Mg from 1.19 to 1.27 Å) while the Mg–O bond is significantly strengthened (from 2.12 to 1.73 Å). However, for dissociation of the CO molecule according to reaction (2), the electron still needs to be transferred to one of the two isoenergetic *p* orbitals of the oxygen ligand in $[MgO]^+$. Optimization of a conical intersection toward these states suggests that this process costs about 5.7 eV (EOM-CCSD/def2TZVP), see Figure S2 for the respective interpolation. Thus, the electron transfer along this decomposition channel is not accessible with the energy available upon excitation into D_3. The dissociation of CO_2 within the excited state, reaction (1*), is likely inaccessible, given the thermal energy calculated as 0.03 eV at 80 K. Curve crossings into the ground state seem unattainable with the available energy as well.

In planar $[Mg(CO_2)(H_2O)]^+$, the weakly bound CO_2 ligand is oriented end-on on the same side of the Mg^+ core as the more strongly bound water molecule. The 3*s* and two 3*p* orbitals are perturbed by the ligands (Fig. 3a), only the 3*p* orbital perpendicular to the molecular plane stays unperturbed: The excitations into the D_1 and D_3 states are shifted to lower energies of 3.28 and 4.70 eV, respectively, the excitation into the D_2 state remains almost unshifted at 3.78 eV.

To investigate how the hydration changes the photochemical activation of CO_2 in the excited state, relaxed CO_2 angle scans for the D_1 and D_2 states are shown in Fig. 3a, b. For D_1, multiple minima are found again, with an almost linear and a bent CO_2 molecule (note that another minimum with bent CO_2 and a very similar energy in D_1 exists with a flipped CO_2 bending angle, see Figure S3 for the respective scan). The D_1 minimum with linear CO_2 has a dramatically different structure compared to the FC point. After promoting the electron from the 3*s* to the 3*p* orbital of Mg^+, the ion linearizes analogously to $[Mg(H_2O)_2]^+$ [47, 49] and the water molecule rotates by 90° to maximize the interaction of the positively charged hydrogen atoms with the electron in the 3*p* orbital of Mg^+, gaining 0.53 eV of internal energy. Contrary to the case without the water ligand, the bent minimum with an activated CO_2^- ligand is now accessible with the energy available after excitation. CO loss from this minimum would only require 2.51 eV for the hydrated case, reaction (5). However, the charge transfer into the *p* orbital

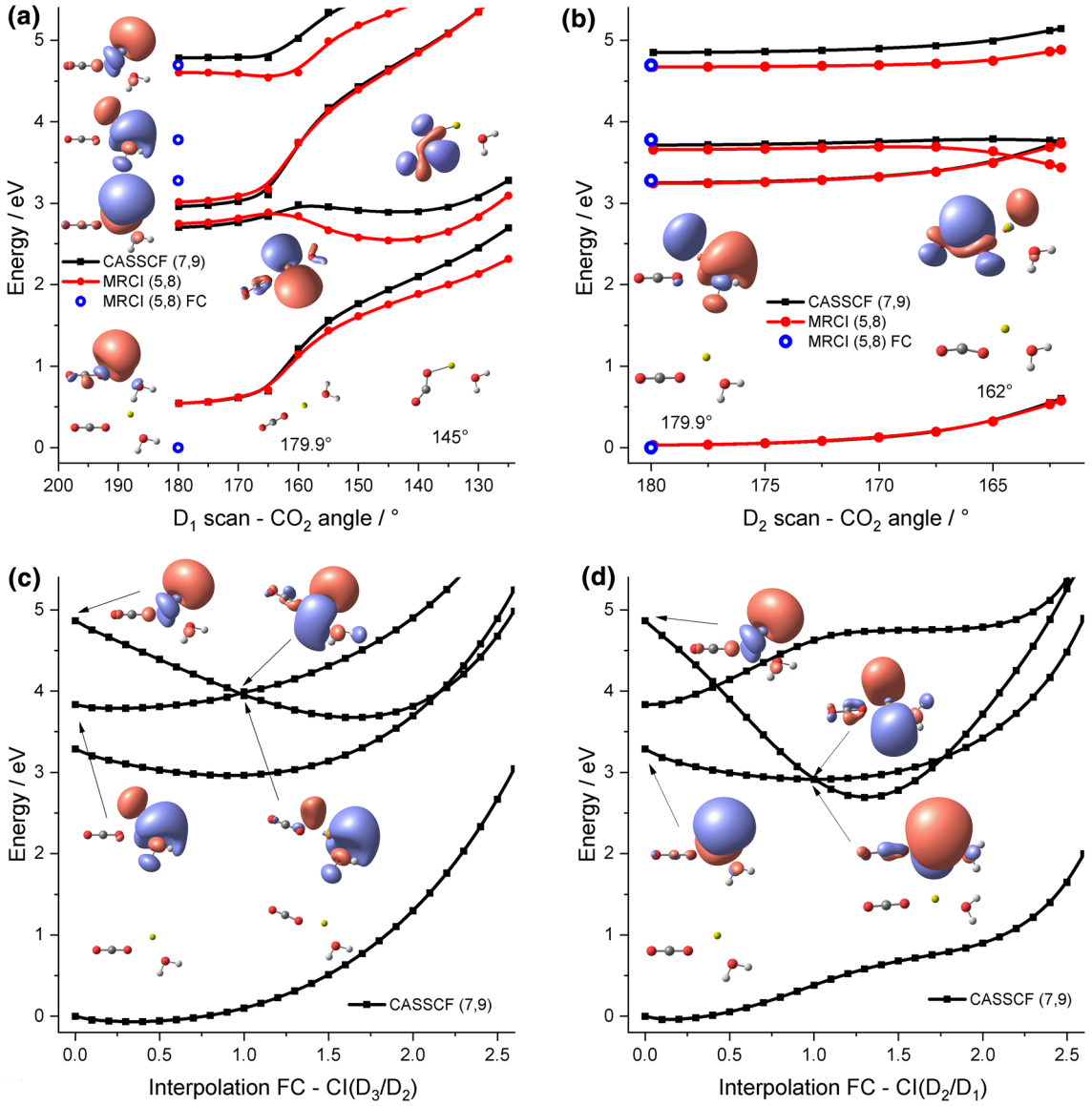

Fig. 3 Relaxed PES scan of the CO_2 angle in $[Mg(CO_2)(H_2O)]^+$ for (**a**) D_1 and (**b**) D_2 at the CASSCF(7,9)/def2-TZVP and MRCI(5,8)//CASSCF(7,9)/def2-TZVP along with the FC point excitation energies at the MRCI(5,8)/def2-TZVP//CCSD/aug-cc-pVDZ level of theory. The structures and the most important singly occupied orbitals according to CASSCF CI vectors are shown for selected structure and states. Interpolation between the FC point and the conical intersection of (**c**) D_3/D_2 and (**d**) D_2/D_1

of the oxygen to access this decomposition channel from D_1 is still very expensive with at least 5.45 eV (EOM-CCSD/def2TZVP), similar to the case without water, see Figure S4 for the respective interpolation. Likewise, decomposition within the excited state manifold is not accessible with the available energy of a single photon, see reaction (3*). Contrary to the case without the water ligand, the gained internal energy after fluorescence from any D_1 minimum is enough for CO_2 evaporation, see reaction (3).

After excitation into D_2, the D_1/D_2 conical intersection can be reached barrierlessly, see Fig. 3b. Again, the antibonding π^* orbital of the carbon dioxide ligand mixes with the occupied $3p$ orbital from Mg^+ in the optimized state upon bending. Afterward, access to a similar bent minimum involving a CO_2^- ligand in the D_1 state can be expected and similar access to decomposition channels with the available energy.

We also investigated the reaction pathways after excitation into the D_3 state and found pathways for direct internal conversion into D_2 and D_1 states (see Fig. 3c, d for interpolations). In both cases, the PES leads monotonically downhill from the FC point to the conical intersections. The orbital analysis of the CIs in Fig. 3c, d shows that for the D_3/D_2 CI, the water molecule and CO_2 rearrange to perturb the

3*p* orbital of Mg^+ which is occupied in D_2 while providing more space for the 3*p* orbital populated in D_3. For the CI into D_1, the two ligands rearrange to provide space for two 3*p* orbitals perpendicular to the molecular axis. However, the ground state is well separated in all scans. The excitation energy into D_3 is sufficient to evaporate a CO_2 molecule from Mg^{*+} via reaction (3*).

The PES scheme in Fig. 4 summarizes our findings. For $[Mg(CO_2)]^+$, excitation into $D_{1,2}$ leads to a bound state where it can only absorb another photon in order to decompose. From the linear D_1 minimum, several higher lying states are resonantly accessible with an excitation energy of 3.2–4.0 eV (EOM-CCSD/aug-cc-pVTZ). These transitions mostly correspond to excitation of the electron into the empty 3*d* orbitals of Mg^+. Internal conversion finally leads to CO_2 loss. Formation of MgO^+ can happen through an intermediate step after excitation from the ground state into D_3. Here, an electron can be transferred from Mg^{*+} to the CO_2 molecule, weakening the C–O bond. However, the observed CO loss is hindered by a significant barrier. Decomposition after internal conversion into the ground state of $[Mg(CO_2)]^+$ can be ruled out as reaction (1) was not observed in the high-energy band in our experiment which should have a significant contribution otherwise. Furthermore, the states are well separated in calculations. Therefore, the CO loss rather takes place photochemically through absorption of an additional photon from the D_1 minimum involving the CO_2^- unit. With the excitation energy, higher lying states are accessible around an excitation energy of about 4.6–4.9 eV (EOM-CCSD/aug-cc-pVTZ). Contrary to the multiphoton excitation in the D_1 minimum with a linear CO_2 molecule, we excite here directly a lone pair electron in the CO_2^- ligand to its out of the bending plane π^* orbital while Mg^{2+} plays a minor role. This explains the different photochemical decomposition pathways in the two experimental bands. Fluorescence or multiphoton excitation into $3p_z$, which requires about 4.5 eV (EOM-CCSD/aug-cc-pVTZ) in the bent D_1 minimum, can explain the partially observed CO_2 loss in the flank of the high energy band previously observed by the group of Duncan [54].

In $[Mg(CO_2)(H_2O)]^+$, CO_2 loss can already happen after fluorescing a photon in the linear D_1 minimum or the D_1 minima with a bent CO_2. Upon excitation into D_2, a CI into D_1 can be accessed allowing similar decomposition pathways. Direct decomposition via CO loss is hindered again by a barrier. Decomposition after internal conversion into the ground state can be ruled out because water loss (reaction (7)) is not observed in our cooled experiment and the ground state is separated from the excited state manifold. Therefore, the $[Mg(CO_2)(OH)]^+$, $[MgO(H_2O)]^+$ and $[Mg(OH)]^+$ fragments observed only with significantly higher laser power and with shifting branching ratios, see Figure S1, occur via multiphoton processes. Excitations into higher lying states are accessible with resonant excitation energies of about 3.6 and 3.5–4.2 eV (EOM-CCSD/aug-cc-pVTZ) in the bent D_1 minimum of Fig. 3a and its flipped version in Figure S3, respectively.

Furthermore, formation of $[Mg(OH)]^+$ as the second most intense channel likely occurs sequentially by absorption of the predominant $[Mg(H_2O)]^+$ fragment as it has an intense absorption band in this range and loses an H atom [47, 49]. Additionally, H loss from the comparable $[Mg(H_2O)_2]^+$ case happens via a multiphoton-process, in line with our interpretation [47, 49].

4 Conclusion

We investigated the photochemistry of $[Mg(CO_2)]^+$ and $[Mg(CO_2)(H_2O)]^+$ as model systems for the role of metal/ligand interactions in the photochemical activation of CO_2 by a combination of ab initio calculations and mass spectrometry experiments in the gas phase. The observed decomposition channels are highly state selective. $[Mg(CO_2)]^+$ loses the CO_2 ligand in the low-energy $3s$–$3p_{x,y}$ band via a multiphoton excitation into the Mg 3*d* shell. With the provided

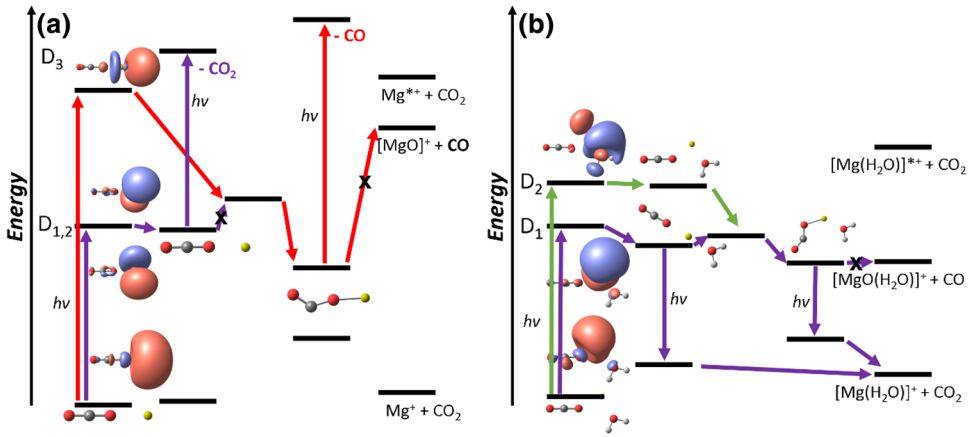

Fig. 4 Simplified reaction scheme illustrating the predominantly observed experimental dissociation channels in Fig. 1 for (**a**) $[Mg(CO_2)]^+$ and (**b**) $[Mg(CO_2)(H_2O)]^+$

energy of the high-energy $3s$–$3p_z$ band, CO_2 is activated through a charge transfer from Mg^{*+} in the excited state manifold and forms a bent CO_2^- ligand on a Mg^{2+} center. This leads to predominant CO loss after absorption of an additional photon by the CO_2^- ligand.

Upon hydration with one water molecule, CO_2 is activated already in the low-energy $3s$–$3p$ band. The rearrangement in the D_1 minima provides enough internal energy for CO_2 loss through fluorescence in addition to the previous multiphoton process. The $[Mg(CO_2)(OH)]^+$, $[MgO(H_2O)]^+$ and $[Mg(OH)]^+$ fragments in the D_2 band arise from an additional excitation in D_1 minima in combination with sequential fragmentation of $[Mg(H_2O)]^+$ to $[Mg(OH)]^+$. For the third $3s$–$3p$ transitions, we predict direct funneling into the first excited state, providing enough energy to directly evaporate a CO_2 molecule on the excited state PES.

Acknowledgements Open access funding provided by Austrian Science Fund (FWF). This work was supported by the Austrian Science Fund (FWF), Project No. P28896. The computational results presented have been achieved using the HPC infrastructure LEO of the University of Innsbruck. The tunable OPO system is part of the Innsbruck Laser Core Facility, financed by the Austrian Federal Ministry of Education, Science and Research.

References

1. Wenderich K, Mul G (2016) Methods, mechanism, and applications of photodeposition in photocatalysis: a review. Chem Rev 116(23):14587–14619. https://doi.org/10.1021/acs.chemrev.6b00327
2. Cheng Y-C, Fleming GR (2009) Dynamics of light harvesting in photosynthesis. Annu Rev Phys Chem 60:241–262. https://doi.org/10.1146/annurev.physchem.040808.090259
3. Middleton CT, de La Harpe K, Su C, Law YK, Crespo-Hernández CE, Kohler B (2009) DNA excited-state dynamics: from single bases to the double helix. Annu Rev Phys Chem 60:217–239. https://doi.org/10.1146/annurev.physchem.59.032607.093719
4. Perun S, Sobolewski AL, Domcke W (2005) Ab initio studies on the radiationless decay mechanisms of the lowest excited singlet states of 9H-adenine. J Am Chem Soc 127(17):6257–6265. https://doi.org/10.1021/ja044321c
5. Bai S, Barbatti M (2017) Spatial factors for triplet fusion reaction of singlet oxygen photosensitization. J Phys Chem Lett 8(21):5456–5460. https://doi.org/10.1021/acs.jpclett.7b02574
6. Bai S, Barbatti M (2017) Divide-to-Conquer: a kinetic model for singlet oxygen photosensitization. J Chem Theory Comput 13(11):5528–5538. https://doi.org/10.1021/acs.jctc.7b00619
7. Martínez-Fernández L, González-Vázquez J, González L, Corral I (2015) Time-resolved insight into the photosensitized generation of singlet oxygen in endoperoxides. J Chem Theory Comput 11(2):406–414. https://doi.org/10.1021/ct500909a
8. Nogueira JJ, Oppel M, González L (2015) Enhancing intersystem crossing in phenotiazinium dyes by intercalation into DNA. Angew Chem Int Ed 54(14):4375–4378. https://doi.org/10.1002/anie.201411456
9. Miyamoto S, Martinez GR, Medeiros MHG, Di Mascio P (2003) Singlet molecular oxygen generated from lipid hydroperoxides by the russell mechanism: studies using 18(O)-labeled linoleic acid hydroperoxide and monomol light emission measurements. J Am Chem Soc 125(20):6172–6179. https://doi.org/10.1021/ja029115o
10. Lischka H, Nachtigallová D, Aquino AJA, Szalay PG, Plasser F, Machado FBC, Barbatti M (2018) Multireference approaches for excited states of molecules. Chem Rev 118(15):7293–7361. https://doi.org/10.1021/acs.chemrev.8b00244
11. Szalay PG, Müller T, Gidofalvi G, Lischka H, Shepard R (2012) Multiconfiguration self-consistent field and multireference configuration interaction methods and applications. Chem Rev 112(1):108–181. https://doi.org/10.1021/cr200137a
12. Helgaker T, Jorgensen P, Olsen J (2014) Molecular electronic-structure theory. Wiley, Chichester
13. Curchod BFE, Martínez TJ (2018) Ab initio nonadiabatic quantum molecular dynamics. Chem Rev 118(7):3305–3336. https://doi.org/10.1021/acs.chemrev.7b00423
14. Levine BG, Martínez TJ (2007) Isomerization through conical intersections. Annu Rev Phys Chem 58:613–634. https://doi.org/10.1146/annurev.physchem.57.032905.104612
15. Domcke W, Yarkony DR, Köppel H (2011) Advanced series in physical chemistry: conical intersections: theory, computation and experiment, vol 17. World Scientific, Singapore
16. Xie C, Malbon CL, Yarkony DR, Xie D, Guo H (2018) Signatures of a conical intersection in adiabatic dissociation on the ground electronic state. J Am Chem Soc 140(6):1986–1989. https://doi.org/10.1021/jacs.7b11489
17. Neese F, Petrenko T, Ganyushin D, Olbrich G (2007) Advanced aspects of ab initio theoretical optical spectroscopy of transition metal complexes: multiplets, spin-orbit coupling and resonance Raman intensities. Coord Chem Rev 251(3–4):288–327. https://doi.org/10.1016/j.ccr.2006.05.019
18. Hellman A, Baerends EJ, Biczysko M, Bligaard T, Christensen CH, Clary DC, Dahl S, van Harrevelt R, Honkala K, Jonsson H et al (2006) Predicting catalysis: understanding ammonia synthesis from first-principles calculations. J Phys Chem B 110(36):17719–17735. https://doi.org/10.1021/jp056982h
19. Behrens M, Studt F, Kasatkin I, Kühl S, Hävecker M, Abild-Pedersen F, Zander S, Girgsdies F, Kurr P, Kniep B-L et al (2012) The active site of methanol synthesis over Cu/ZnO/Al_2O_3 industrial catalysts. Science 336(6083):893–897. https://doi.org/10.1126/science.1219831
20. Smith NA, Sadler PJ (2013) Photoactivatable metal complexes: from theory to applications in biotechnology and medicine. Philos Trans A Math Phys Eng Sci 371(1995):20120519. https://doi.org/10.1098/rsta.2012.0519
21. Schwarz H (2017) Ménage-à-trois: single-atom catalysis, mass spectrometry, and computational chemistry. Catal Sci Technol 7(19):4302–4314. https://doi.org/10.1039/C6CY02658C
22. Schwarz H (2017) Metal-mediated activation of carbon dioxide in the gas phase: mechanistic insight derived from a combined experimental/computational approach. Coord Chem Rev 334:112–123. https://doi.org/10.1016/j.ccr.2016.03.009

23. Álvarez A, Bansode A, Urakawa A, Bavykina AV, Wezendonk TA, Makkee M, Gascon J, Kapteijn F (2017) Challenges in the greener production of formates/formic acid, methanol, and DME by heterogeneously catalyzed CO_2 hydrogenation processes. Chem Rev 117(14):9804–9838. https://doi.org/10.1021/acs.chemrev.6b00816
24. Gutsev GL, Bartlett RJ, Compton RN (1998) Electron affinities of CO_2, OCS, and CS_2. J Chem Phys 108(16):6756–6762. https://doi.org/10.1063/1.476091
25. Cooper CD, Compton RN (1972) Metastable anions of CO_2. Chem Phys Lett 14(1):29–32. https://doi.org/10.1016/0009-2614(72)87133-1
26. Sommerfeld T, Meyer H-D, Cederbaum LS (2004) Potential energy surface of the CO_2^- anion. Phys Chem Chem Phys 6(1):42. https://doi.org/10.1039/b312005h
27. Aresta M, Dibenedetto A (2007) Utilisation of CO_2 as a chemical feedstock: opportunities and challenges. Dalton Trans 28:2975–2992. https://doi.org/10.1039/b700658f
28. Herburger A, Ončák M, Siu C-K, Demissie EG, Heller J, Tang WK, Beyer MK (2019) Infrared spectroscopy of size-selected hydrated carbon dioxide radical anions $CO_2^-(H_2O)_n$ ($n = 2$–61) in the C–O stretch region. Chem Eur J 25:10165–10171. https://doi.org/10.1002/chem.201901650
29. Habteyes T, Velarde L, Sanov A (2007) Photodissociation of CO_2^- in water clusters via Renner–Teller and conical interactions. J Chem Phys 126(15):154301. https://doi.org/10.1063/1.2717932
30. Habteyes T, Velarde L, Sanov A (2006) Solvent-enabled photodissociation of CO_2^- in water clusters. Chem Phys Lett 424(4–6):268–272. https://doi.org/10.1016/j.cplett.2006.04.070
31. Weber JM (2014) The interaction of negative charge with carbon dioxide—insight into solvation, speciation and reductive activation from cluster studies. Int Rev Phys Chem 33(4):489–519. https://doi.org/10.1080/0144235X.2014.969554
32. Barwa E, Pascher TF, Ončák M, van der Linde C, Beyer MK (2020) Carbon dioxide activation at metal centers: evolution of charge transfer from $Mg^{\cdot+}$ to CO_2 in $[MgCO_2(H_2O)]_n^+$, $n = 0$–8. Angew Chem Int Ed 59:7467–7471. https://doi.org/10.1002/anie.202001292
33. Barwa E, Ončák M, Pascher TF, Taxer T, van der Linde C, Beyer MK (2019) CO_2/O_2 exchange in magnesium-water clusters $Mg^+(H_2O)_n$. J Phys Chem A 123:73–81. https://doi.org/10.1021/acs.jpca.8b10530
34. Roithová J (2012) Characterization of reaction intermediates by ion spectroscopy. Chem Soc Rev 41(2):547–559. https://doi.org/10.1039/c1cs15133a
35. Pascher TF, Ončák M, van der Linde C, Beyer MK (2020) UV/VIS spectroscopy of copper formate clusters: insight into metal-ligand photochemistry. Chem Eur J. https://doi.org/10.1002/chem.202000280 (**In print**)
36. Pascher TF, Ončák M, van der Linde C, Beyer MK (2019) Release of formic acid from copper formate: hydride, proton-coupled electron and hydrogen atom transfer all play their role. ChemPhysChem 20(11):1420–1424. https://doi.org/10.1002/cphc.201900095
37. Pascher TF, Ončák M, van der Linde C, Beyer MK (2019) Decomposition of copper formate clusters: insight into elementary steps of calcination and carbon dioxide activation. ChemistryOpen 8:1453–1459. https://doi.org/10.1002/open.201900282
38. Watanabe H, Iwata S, Hashimoto K, Misaizu F, Fuke K (1995) Molecular-orbital studies of the structures and reactions of singly charged magnesium-ion with water clusters, $Mg^+(H_2O)_n$. J Am Chem Soc 117(2):755–763. https://doi.org/10.1021/ja00107a019
39. Berg C, Beyer M, Achatz U, Joos S, Niedner-Schatteburg G, Bondybey VE (1998) Stability and reactivity of hydrated magnesium cations. Chem Phys 239(1–3):379–392. https://doi.org/10.1016/S0301-0104(98)00278-X
40. van der Linde C, Akhgarnusch A, Siu C-K, Beyer MK (2011) Hydrated magnesium cations $Mg^+(H_2O)_n$, $n \approx 20$–60, exhibit chemistry of the hydrated electron in reactions with O_2 and CO_2. J Phys Chem A 115:10174–10180. https://doi.org/10.1021/jp206140k
41. Reinhard BM, Lagutschenkov A, Niedner-Schatteburg G (2004) Ab initio study of [Mg, $n H_2O$]- reactive decay products: structure and stability of magnesium oxide and magnesium hydroxide water cluster anions $[MgO,(n-1)H_2O]^-$, $[HMgOH,(n-1)H_2O]^-$ and $[Mg(OH)_2,(n-2)H_2O]^-$. Phys Chem Chem Phys 6(17):4268–4275. https://doi.org/10.1039/b405747c
42. Reinhard BM, Niedner-Schatteburg G (2002) Co-existence of hydrated electron and metal Di-cation in $[Mg(H_2O)_n]^+$. Phys Chem Chem Phys 4(8):1471–1477. https://doi.org/10.1039/b109774c
43. Reinhard BM, Niedner-Schatteburg G (2003) Ab initio treatment of magnesium water cluster anions [Mg, $n H_2O]^-$, $n \leq 11$. Phys Chem Chem Phys 5(10):1970–1980. https://doi.org/10.1039/b302254d
44. Siu C-K, Liu ZF (2005) Reaction mechanisms for size-dependent H loss in $Mg^+(H_2O)_n$: solvation controlled electron transfer. Phys Chem Chem Phys 7(5):1005–1013. https://doi.org/10.1039/b418787n
45. Siu C-K, Liu ZF (2002) Ab initio studies on the mechanism of the size-dependent hydrogen-loss reaction in $Mg^+(H_2O)_n$. Chem Eur J 8(14):3177–3186. https://doi.org/10.1002/1521-3765(20020715)8:14%3c3177:AID-CHEM3177%3e3.0.CO;2-B
46. Asada T, Iwata S (1996) Hybrid procedure of ab initio molecular orbital calculation and monte carlo simulation for studying intracluster reactions: applications to $Mg^+(H_2O)_n$ ($n = 1$–4). Chem Phys Lett 260(1–2):1–6. https://doi.org/10.1016/0009-2614(96)00886-X
47. Ončák M, Taxer T, Barwa E, van der Linde C, Beyer MK (2018) Photochemistry and spectroscopy of small hydrated magnesium clusters $Mg^+(H_2O)_n$, $n = 1$–5. J Chem Phys 149(4):44309. https://doi.org/10.1063/1.5037401
48. Taxer T, Ončák M, Barwa E, van der Linde C, Beyer MK (2019) Electronic spectroscopy and nanocalorimetry of hydrated magnesium ions $[Mg(H_2O)_n]^+$, $n = 20$–70: spontaneous formation of a hydrated electron? Faraday Discuss 217:584–600. https://doi.org/10.1039/C8FD00204E
49. Misaizu F, Sanekata M, Fuke K, Iwata S (1994) Photodissociation study on $Mg^+(H_2O)_n$, $n = 1$–5: electronic structure and photoinduced intracluster reaction. J Chem Phys 100(2):1161–1170. https://doi.org/10.1063/1.466646
50. Willey KF, Yeh CS, Robbins DL, Pilgrim JS, Duncan MA (1992) Photodissociation spectroscopy of Mg^+–H_2O and Mg^+–D_2O. J Chem Phys 97(12):8886–8895. https://doi.org/10.1063/1.463363
51. Yeh CS, Willey KF, Robbins DL, Pilgrim JS, Duncan MA (1992) Photodissociation spectroscopy of Mg^+–H_2O. Chem Phys Lett 196(3–4):233–238. https://doi.org/10.1016/0009-2614(92)85960-I
52. Bauschlicher CW, Partridge H (1991) A determination of Mg^+—ligand binding energies. J Phys Chem 95(10):3946–3950. https://doi.org/10.1021/j100163a011
53. Bauschlicher CW, Partridge H (1991) Mg^+ ligand binding energies. Chem Phys Lett 181(2–3):129–133. https://doi.org/10.1016/0009-2614(91)90344-9
54. Yeh CS, Willey KF, Robbins DL, Pilgrim JS, Duncan MA (1993) Photodissociation spectroscopy of the Mg^+–CO_2 complex and its isotopic analogs. J Chem Phys 98(3):1867–1875. https://doi.org/10.1063/1.464221
55. Yeh CS, Willey KF, Robbins DL, Duncan MA (1994) Photodissociation of magnesium ion/molecule complexes in a reflectron time-of-flight mass spectrometer. Int J Mass Spectrom Ion Process

131(Supplement C):307–317. https://doi.org/10.1016/0168-1176(93)03872-j
56. Yeh CS, Willey KF, Robbins DL, Duncan MA (1992) Photoinduced reaction in collinear aligned magnesium(1^+)-carbon dioxide complexes. J Phys Chem 96(20):7833–7836. https://doi.org/10.1021/j100199a001
57. Barone V, Bloino J, Biczysko M, Santoro F (2009) Fully integrated approach to compute vibrationally resolved optical spectra: from small molecules to macrosystems. J Chem Theory Comput 5(3):540–554. https://doi.org/10.1021/ct8004744
58. Santoro F, Improta R, Lami A, Bloino J, Barone V (2007) Effective method to compute Franck–Condon integrals for optical spectra of large molecules in solution. J Chem Phys 126(8):84509. https://doi.org/10.1063/1.2437197
59. Schinke R (1993) Photodissociation dynamics: spectroscopy and fragmentation of small polyatomic molecules. Cambridge monographs on atomic molecular and chemical physics, vol 1. Cambridge University Press, Cambridge
60. Lee SY, Brown RC, Heller EJ (1983) Multidimensional reflection approximation: application to the photodissociation of polyatomics. J Phys Chem 87(12):2045–2053. https://doi.org/10.1021/j100235a006
61. Ončák M, Šištík L, Slavíček P (2010) Can theory quantitatively model stratospheric photolysis? Ab initio estimate of absolute absorption cross sections of ClOOCl. J Chem Phys 133(17):174303. https://doi.org/10.1063/1.3499599
62. Frisch MJ, Trucks GW, Schlegel HB, Scuseria GE, Robb MA, Cheeseman JR, Scalmani G, Barone V, Petersson GA, Nakatsuji H et al (2016) Gaussian 16, Revision A.03. Gaussian Inc., Wallingford
63. Werner H-J, Knowles PJ, Lindh R et al (2009) MOLPRO, version 2009.1, a package of ab initio programs
64. Werner H-J, Knowles PJ, Knizia G, Manby FR, Schütz M (2012) Molpro: a general-purpose quantum chemistry program package. WIREs Comput Mol Sci 2(2):242–253. https://doi.org/10.1002/wcms.82